Schemes for the observation of photon correlation functions in circuit QED with linear detectors

Marcus P. da Silva,[1] Deniz Bozyigit,[2] Andreas Wallraff,[2] and Alexandre Blais[1]
[1]*Département de Physique, Université de Sherbrooke, Sherbrooke, Québec, Canada, J1K 2R1*
[2]*Department of Physics, ETH Zürich, CH-8093, Zürich, Switzerland*
(Received 7 June 2010; published 5 October 2010)

Correlations are important tools in the characterization of quantum fields, as they can be used to describe statistical properties of the fields, such as bunching and antibunching, as well as to perform field state tomography. Here we analyze experiments by Bozyigit *et al.* [Nat. Phys. (to appear), e-print arXiv:1002.3738] where correlation functions can be observed using the measurement records of linear detectors (i.e., quadrature measurements), instead of relying on intensity or number detectors. We also describe how large amplitude noise introduced by these detectors can be quantified and subtracted from the data. This enables, in particular, the observation of first- and second-order coherence functions of microwave photon fields generated using circuit quantum electrodynamics and propagating in superconducting transmission lines under the condition that noise is sufficiently low.

DOI: 10.1103/PhysRevA.82.043804 PACS number(s): 42.50.Ct, 42.50.Pq, 78.20.Bh, 42.50.Lc

I. INTRODUCTION

Field correlations are widely used in the characterization of classical and quantum fields [1,2]. A particular set of correlations used for such purposes are the coherence functions of a field, as described by Glauber [3–5]. These functions can be used to quantify the ability of a field to interfere with itself, as well as to demonstrate features of quantum fields which cannot be reproduced in a classical system. One of the most famous of these quantum phenomena is known as *antibunching* [6,7], and it is frequently used to characterize single-photon sources in the optical regime [8–12]. Over the recent years Josephson-junction-based superconducting circuits, resonators, and transmission lines have emerged as a platform for performing quantum optics experiments in the microwave regime [13–23]. While in the optical regime coherence functions are usually measured using an interferometer where photon number detectors are used, in the microwave regime, linear detectors (i.e., field quadrature measurements) are ubiquitous due to the difficulty of building reliable photon number detectors. This raises the question of how to measure field correlations using linear detectors. This paper answers this question by generalizing the approach of Grosse *et al.* [24], and describing the theory behind the recent experiments performed by Bozyigit *et al.* [25], where correlations of a propagating microwave field are measured using only linear detectors instead of intensity detectors. While the discussion here focuses on the measurement of first- and second-order coherence functions of microwave fields, the analysis can be applied to any correlation of field operators. We note that the measurement of correlation functions of propagating microwave fields using nonlinear (i.e., square-law) detectors was theoretically studied in Ref. [26], under the assumption of negligible correlation in the noise added by the detection chain. In practice, these correlations turn out to be important and are discussed here. Recent work by Menzel *et al.* [27] and Mariantoni *et al.* [28] is in a similar direction to the work presented here.

The paper is organized as follows. Section II gives a brief review of coherence functions and how they are measured with nonlinear detectors. Section III describes how field correlations and, in particular, coherence functions can be measured using linear detectors. Section IV describes the effects of noise in the experiments, and finally Sec. V describes how the experimental setup can be simplified in circuit quantum-electrodynamics (QED) experiments.

II. COHERENCE FUNCTIONS

The meaning of *coherence* of a field in a single frequency mode, with corresponding annihilation operator $\hat{a}$, can be understood by considering interference experiments which use the field leaking out of this mode. Using a double slit, the field can be made to travel two pathways of different lengths which terminate at a single pointlike photon detector, as depicted in Fig. 1(a). The combined field that impinges on the detector is made up of fields originally emitted at times t and $t+\tau$ (which depend on the lengths of the paths), so that the observed field intensity at the detector is the sum of the intensities of the two fields plus an interference term which depends on $\langle\hat{a}^\dagger(t)\hat{a}(t+\tau)\rangle$ [1]. Interference effects can only be observed if this correlation is nonzero. It is therefore natural to define

$$G^{(1)}(t,t+\tau)=\langle\hat{a}^\dagger(t)\hat{a}(t+\tau)\rangle, \tag{1}$$

which is called the *first-order coherence function* [3], as a measure of the emitted field's potential to interfere with itself—in other words, a measure of the coherence of the field. One may also consider

$$G^{(1)}(\tau)=\int_{\mathcal{I}} dt\, G^{(1)}(t,t+\tau), \tag{2}$$

for some time interval $\mathcal{I}$ in order to obtain an expression that depends only on the time difference between the two paths. If $G^{(1)}(\tau)=0$, no interference effects can be observed for a path difference of $c\tau$, where c is the speed of light.

The measure of coherence that is most often used to distinguish classical fields from quantum fields is the *second-order coherence function* given by

$$G^{(2)}(t,t+\tau)=\langle\hat{a}^\dagger(t)\hat{a}^\dagger(t+\tau)\hat{a}(t+\tau)\hat{a}(t)\rangle, \tag{3}$$

or by the integrated version,

$$G^{(2)}(\tau)=\int_{\mathcal{I}} dt\, G^{(2)}(t,t+\tau). \tag{4}$$

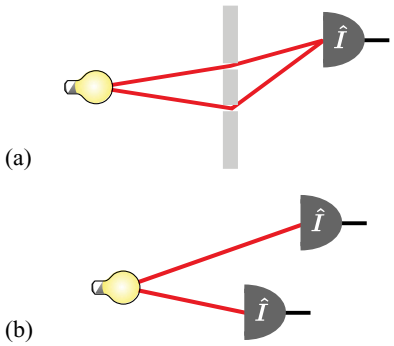

FIG. 1. (Color online) Experimental setups illustrating different degrees of optical coherence with intensity detectors. The red lines represent quantum fields, and the black lines represent measurement records.

The canonical experiment which gives the physical interpretation of $G^{(2)}$ is one with a single light source and two pointlike detectors, such that the field takes a time t and $t+\tau$, respectively, to reach each detector, as depicted in Fig. 1(b). In that case the correlation between the detected intensities is given by $G^{(2)}(t,t+\tau)$.

For classical fields, where the field operator in the expressions above are replaced by c numbers, one finds that $|G^{(2)}(0)| \geqslant |G^{(2)}(\tau)|$, while there are quantum states of the field that yield $|G^{(2)}(0)| < |G^{(2)}(\tau)|$ for $\tau \neq 0$, a phenomenon known as *antibunching* [6,7]. The canonical examples of antibunched field states are single-photon states and squeezed states. In the case of pulsed experiments—where the light field state is prepared with a repetition period of t_p—one writes instead that classical fields obey $|G^{(2)}(0)| \geqslant |G^{(2)}(kt_p)|$, and that some quantum states of the field yield $|G^{(2)}(0)| < |G^{(2)}(kt_p)|$ for $k \neq 0$. Only pulsed experiments will be considered in the remainder of this paper, the generalization to continuous experiments being straightforward.

A. Standard experimental setups

As illustrated in Fig. 2, we consider experiments where the source is a single mode of a cavity coupled to a transmission line via a leaky mirror, a situation typical of cavity QED [29–31]. In circuit QED, for example, arbitrary superpositions of a single photon and vacuum can be prepared in the dispersive regime via Purcell decay [16] or by strong coupling to a qubit brought into resonance with the cavity [25], although details of the state preparation are not important for the remainder of the discussion. The harmonic field in the cavity is associated with an annihilation operators $\hat{a}$ with the usual same-time commutation relation $[\hat{a},\hat{a}^\dagger] = \mathbb{1}$. Using input-output theory [2,32–34], one can show that $\hat{a}$ is related to the modes of the transmission line via

$$\hat{b}_{\rm out}(t) = \sqrt{\kappa_b}\hat{a}(t) - \hat{b}_{\rm in}(t), \tag{5}$$

where κ_b is the rate at which photons leak out of $\hat{a}$, and the input and output fields are given by

$$\hat{b}_{\rm in}(t) = \frac{1}{\sqrt{2\pi}}\int_{-\infty}^{+\infty} d\omega\, e^{-i\omega(t-t_0)} b(t_0,\omega), \tag{6}$$

$$\hat{b}_{\rm out}(t) = \frac{1}{\sqrt{2\pi}}\int_{-\infty}^{+\infty} d\omega\, e^{-i\omega(t-t_1)} b(t_1,\omega). \tag{7}$$

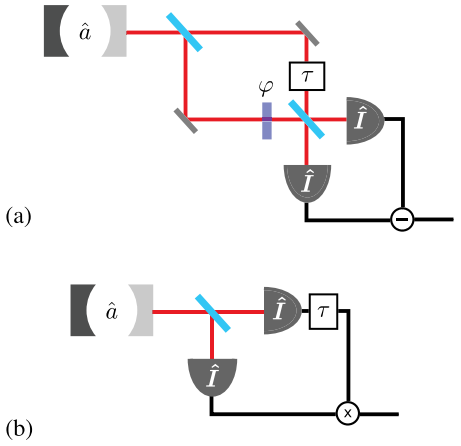

FIG. 2. (Color online) Standard experiments for the observation of $G^{(1)}$ and $G^{(2)}$ using intensity detectors: (a) a Mach-Zender interferometer with a variable delay τ and a variable phase shift φ, and (b) a Hanbury Brown and Twiss (HBT) interferometer with a variable delay τ. The light-blue components are balanced beam splitters. The cavity is taken to be one-sided, with one mirror being perfectly reflective.

for transmission line modes $b(t,\omega)$ at times $t_0 < t < t_1$, and correspond to fields propagating toward or away from the cavity. The commutation relations of the input and output fields are given by

$$[\hat{b}_{\rm in}(t),\hat{b}^\dagger_{\rm in}(t+\tau)] = [\hat{b}_{\rm out}(t),\hat{b}^\dagger_{\rm out}(t+\tau)] = \delta(\tau). \tag{8}$$

These definitions lead to an equation of motion for $\hat{a}$ in the interaction frame to be given, for a one-sided cavity, by

$$\dot{\hat{a}}(t) = -\frac{\kappa_b}{2}\hat{a}(t) + \sqrt{\kappa_b}\hat{b}_{\rm in}(t). \tag{9}$$

From Eq. (5) it is clear that the correlations of $\hat{b}_{\rm out}$ are proportional to the correlations of $\hat{a}$ when $\hat{b}_{\rm in}$ is prepared in the vacuum state. The remainder of the discussion will focus on the observation of the coherence functions of the output field $\hat{b}_{\rm out}$ only, as they can be taken to be equivalent to the correlation functions of $\hat{a}$. The "out" subscript will also be dropped when it is clear from the context.

The state of the cavity field is taken to be prepared at times $t = kt_p$ for integer k and repetition period t_p, and allowed to decay via the leaky mirror as described above. The repetition period is chosen to obey $t_p \gg 2\pi/\kappa_b$ so that the cavity can be taken to be in equilibrium at the time of the next preparation of the cavity field.

When working with photons in the optical frequencies, $G^{(1)}$ is usually observed using a Mach-Zender interferometer with a variable delay of τ in one of the branches [35], as depicted in Fig. 2(a). The difference between the intensities in the photocurrent detectors can yield the real or the imaginary part of $G^{(1)}$, depending on the phase shift φ in the lower branch. The standard approach to the observation of $G^{(2)}$ is to use a Hanbury Brown and Twiss (HBT) interferometer [35], which is illustrated in Fig. 2(b). In order to observe $G^{(2)}$, one simply measures the correlations between the photocurrents of the two detectors.

Both these setups rely on field intensity detectors, which give information about the number of photons, and thus can

be modeled by nonlinear quantum optical interactions.[1] Low-noise intensity detectors for optical fields are common, and although nonlinear detectors have been demonstrated in the microwave regime [16,36] (albeit with higher noise levels than in optics), the main motivation for this paper is to illustrate how the coherence functions of microwave fields in circuit QED may be measured through the use of linear detectors only.

III. LINEAR DETECTORS

Field quadrature measurements of microwave signals is a standard technique [37] which has been applied very successfully to quantum electrical circuits in recent years to demonstrate, for example, new regimes of cavity QED [13], high-contrast detection of qubit states [38], photon states [14], and nanomechanical oscillator states [39]. Since field quadrature operators are fundamentally different from number operators, different experimental setups are required in order to measure the coherence functions $G^{(1)}$ and $G^{(2)}$. Grosse *et al.* [24] have demonstrated how HBT interferometers can be modified to measure $G^{(2)}$ using field quadratures instead of intensity measurements. Here we analyze similar experiments [25], and consider generalizations and simplifications which exploit features of circuit QED, while at the same time considering the large added noise due to the high-electron-mobility transistor (HEMT) amplifiers currently required for measurement in this system.

The details of the implementation of quadrature operator measurements in the microwave regime are different from the standard optical implementation. In particular, homodyne detection in the microwave regime is performed via mixing instead of beam splitting [37]. For simplicity we will, however, consider the optical analogs of the devices we discuss. Common nonidealities in the microwave regime, such as weak thermal states instead of vacuum inputs, can be treated straightforwardly by considering different input states, and thus do not change the analysis significantly.

The measurement of both quadratures of a propagating field, realized in optics through eight-port homodyne [40] or heterodyne detection, is performed by an in-phase–quadrature (IQ) mixer in the microwave regime [37]. The symbol for the IQ mixer, and its description in terms of its optical analog are depicted in Fig. 3. The input is any propagating quantum field with annihilation operator $\hat{r}$, which may stand for any propagating field considered in this paper. The outputs are quadrature measurements of the superpositions of the $\hat{r}$ field with a mode $\hat{v}_r$ in the vacuum state, where $[\hat{r},\hat{v}_r^\dagger]=0$. These outputs are labeled X_1 and P_2 to emphasize that the measurements are made on different commuting modes, and correspond to the in-phase component and the quadrature component of the measurement, respectively.

Finally, it is important to note that, for most circuit QED experiments, only averages of these quadratures over many realizations of the experiment are measured. Here, however, we are interested in experiments where the full time records

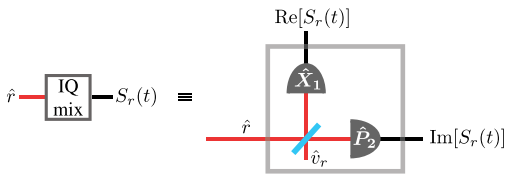

FIG. 3. (Color online) Optical analog of an IQ mixer as an eight-port homodyne detector. The field $\hat{r}$ is fed into a balanced beam splitter along with vacuum $\hat{v}_r$. The $\hat{X}$ quadrature of one of the beam-splitter outputs is measured while the $\hat{P}$ quadrature of the other output is measured. The classical outcomes are the real and imaginary parts of the complex envelope $S_r(t)$.

of these quadratures are recorded, for each realization of the experiments [25]. Based on these full records, any averages or correlation functions can be reconstructed, as is discussed in the next sections.

A. Complex envelope

Given the two classical outputs $X_1(t)$ and $P_2(t)$, it is useful to define the complex envelope $S_r(t)$ of $\hat{r}$ as

$$S_r(t) = X_1(t) + i\,P_2(t), \tag{10}$$

which is a random c number due to the dependence on the measurement records of the quadratures. Noting that

$$\langle X_1(t)\rangle = \left\langle \frac{\hat{r}_1+\hat{r}_1^\dagger}{\sqrt{2}}\right\rangle = \langle \hat{X}_r(t)\rangle + \langle \hat{X}_v(t)\rangle, \tag{11}$$

$$\langle P_2(t)\rangle = -i\left\langle \frac{\hat{r}_2-\hat{r}_2^\dagger}{\sqrt{2}}\right\rangle = \langle \hat{P}_r(t)\rangle - \langle \hat{P}_v(t)\rangle, \tag{12}$$

one may write that $\langle S_r(t)\rangle = \langle \hat{S}_r(t)\rangle$, where the complex envelope operator $\hat{S}_r$ is defined by

$$\hat{S}_r(t) \equiv \hat{r}(t) + \hat{v}_r^\dagger(t) = \hat{X}_1(t) + i\,\hat{P}_2(t). \tag{13}$$

In order to simplify the remainder of the calculations, it is convenient to define $\hat{S}_r$ in this manner instead of using the quadrature operators explicitly.

Given that the mode $\hat{v}_r$ is in the vacuum state, the expression for the expectation values takes simple forms. The presence of the vacuum mode $\hat{v}_r$ is indeed important as it leads to the commutation relation,

$$[\hat{S}_r(t),\hat{S}_r^\dagger(t')] = 0, \tag{14}$$

implying that $\hat{S}_r$ is normal and therefore diagonalizable. Since $\hat{S}_r$ is described by the sum of the commuting operators $\hat{X}_1$ and $\hat{P}_2$, its eigenvalues are given by the sum of the eigenvalues of these operators for any fixed eigenvector. This corresponds to the measurement record S_r of $\hat{S}_r$ being simply the sum of the measurement records X_1 and P_2, as claimed earlier. Note that this does *not* imply that both quadratures of $\hat{r}$ can be measured simultaneously without back-action.

Since $\hat{S}_r$ and $\hat{S}_r^\dagger$ commute at all times, arbitrary correlations of these operators, like the correlations of their measurement records, do not depend on operator ordering. Therefore,

$$\left\langle (S_r^*)^m S_r^n\right\rangle = \left\langle (\hat{S}_r^\dagger)^m \hat{S}_r^n\right\rangle = \langle (\hat{r}^\dagger+\hat{v}_r)^m(\hat{r}+\hat{v}_r^\dagger)^n\rangle, \tag{15}$$

[1]Linearity in this sense refers to the representability of the Heisenberg picture evolution by a linear transformation of creation and annihilation operators for all times.

independently of the ordering of the terms. However, in order to reduce these expressions to a correlation function of $\hat{r}$ alone, one must rewrite the expression such that the $\hat{v}_r$ modes are in normal ordering in order to immediately evaluate the expectation values, leading to

$$\left\langle (S_r^*)^m S_r^n \right\rangle = \left\langle (\hat{S}_r^\dagger)^m \hat{S}_r^n \right\rangle = \langle \hat{r}^n (\hat{r}^\dagger)^m \rangle, \tag{16}$$

or in other words, correlations of the complex envelope of a field correspond to antinormally ordered correlations of the field operator, under the assumption that the $\hat{v}_r$ mode is prepared in the vacuum. In this case, the measurement of $\hat{S}_r$ is described by the Husimi-Kano Q function which is known to give access to antinormally ordered same-time correlations [40–42]. Similar results hold for multitime correlations.

If instead of having the $\hat{v}_r$ mode in the vacuum state one has a thermal state, Eq. (16) is modified by the addition of $\min(m,n)$ terms since $\langle (\hat{v}_r^\dagger)^m \hat{v}_r^n \rangle \propto \delta_{mn}$ for a thermal state. This simply leads to additional noise correlation terms in the discussion that follows, which can be taken care of with minor modifications. The effect of thermal excitations on the input state can also be handled straightforwardly, as discussed in Appendix A.

It is important to note that, while arbitrary correlations can be evaluated with this approach, the number of statistical samples needed to obtain a desired precision in the estimate grows as the noise power raised to the desired correlation order (see Appendix B for details). In practice, this limits the order of the correlations measured with current amplifier noise levels due to the large number of repetitions of the experiment needed to obtain reasonable error bars. Use of quantum limited amplifiers would greatly improve the situation [20,21,43].

B. $G^{(1)}$ observation

As depicted in Fig. 4, with IQ mixers, the first-order correlation function $G^{(1)}$ can be measured from the outputs of an HBT interferometer. Because of the unitarity of the beam splitter and the presence of a vacuum port, the complex envelope operators of the outputs labeled $\hat{c}$ and $\hat{d}$ commute.

The autocorrelation of one of the complex envelopes, say $S_c(t)$, is given by

$$\Gamma_\alpha^{(1)}(t,t+\tau) = \langle \hat{S}_c^\dagger(t)\hat{S}_c(t+\tau)\rangle = \delta(\tau) + \tfrac{1}{2}\langle \hat{b}^\dagger(t)\hat{b}(t+\tau)\rangle, \tag{17}$$

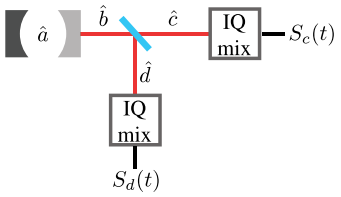

FIG. 4. (Color online) Hanbury Brown and Twiss interferometer with complex envelope measurement used to measure the first-order coherence function $G^{(1)}$. The output of the cavity field is separated by an on-chip beam splitter and the resulting fields measured by an IQ mixer.

while the cross-correlation between the complex envelopes is

$$\Gamma_\beta^{(1)}(t,t+\tau) = \langle \hat{S}_c^\dagger(t)\hat{S}_d(t+\tau)\rangle = \tfrac{1}{2}\langle \hat{b}^\dagger(t)\hat{b}(t+\tau)\rangle, \tag{18}$$

where we have used the fact that the expectation values of all the vacuum modes are zero. Thus, the first-order coherence function $G^{(1)}$ of the $\hat{b}$ field is immediately accessible from cross-correlations of the complex envelopes in a modified HBT interferometer via

$$\begin{aligned} G^{(1)}(t,t+\tau) &= 2\Gamma_\alpha^{(1)}(t,t+\tau) - 2\delta(\tau), \\ &= 2\Gamma_\beta^{(1)}(t,t+\tau), \end{aligned} \tag{19}$$

up to nonidealities, such as amplifier noise, which will be treated later. The exact expressions for $G^{(1)}$ of the states prepared in Ref. [25] are given in Appendix C.

Although the divergence of the δ functions may appear problematic, in reality, due to the finite bandwidth of the experiments, these δ functions are replaced by smooth bounded functions, while the coherence functions are distorted by a convolution kernel which preserves the relative heights of the peaks in the experiment. This results in the filtered correlation functions,

$$\begin{aligned} \Gamma_{\alpha,\mathrm{fil}}^{(1)}(\tau) &= \tfrac{1}{2}G_{\mathrm{fil}}^{(1)}(\tau) + f_{\mathrm{eff}}(\tau), \\ \Gamma_{\beta,\mathrm{fil}}^{(1)}(\tau) &= \tfrac{1}{2}G_{\mathrm{fil}}^{(1)}(\tau), \end{aligned} \tag{20}$$

where $G_{\mathrm{fil}}^{(1)}(\tau) = G^{(1)}(\tau) \ast f_{\mathrm{eff}}(\tau)$ and f_{eff} is a function describing the effective action of the filter (see Appendix D for details).

C. $G^{(2)}$ observation

The expressions needed to measure the second-order coherence function from the complex envelopes can be constructed by inspection of Eq. (13). Depending on which factors are taken to be complex conjugates or to be displaced in time by τ, different correlations can be used to extract information about $G^{(2)}$. One such choice is

$$\begin{aligned} \Gamma_\alpha^{(2)}(t,t+\tau) &= \langle \hat{S}_c^\dagger(t)\hat{S}_d^\dagger(t+\tau)\hat{S}_d(t+\tau)\hat{S}_c(t)\rangle \\ &= \delta^2(0) + \tfrac{1}{2}\langle \hat{b}^\dagger(t)\hat{b}(t)\rangle\delta(0) \\ &\quad + \tfrac{1}{2}\langle \hat{b}^\dagger(t+\tau)\hat{b}(t+\tau)\rangle\delta(0) \\ &\quad + \tfrac{1}{4}\langle \hat{b}^\dagger(t)\hat{b}^\dagger(t+\tau)\hat{b}(t+\tau)\hat{b}(t)\rangle, \end{aligned} \tag{21}$$

so that $G^{(2)}$ can be obtained immediately via

$$\begin{aligned} G^{(2)}(t,t+\tau) &= 4\Gamma_\alpha^{(2)}(t,t+\tau) - 2G^{(1)}(t,t)\delta(0) \\ &\quad - 2G^{(1)}(t+\tau,t+\tau)\delta(0) - 4\delta^2(0). \end{aligned} \tag{22}$$

Another choice that leads more directly to $G^{(2)}$ is

$$\begin{aligned} \Gamma_\beta^{(2)}(t,t+\tau) &= \langle \hat{S}_c^\dagger(t)\hat{S}_c^\dagger(t+\tau)\hat{S}_d(t+\tau)\hat{S}_d(t)\rangle, \\ &= \tfrac{1}{4}\langle \hat{b}^\dagger(t)\hat{b}^\dagger(t+\tau)\hat{b}(t+\tau)\hat{b}(t)\rangle, \end{aligned} \tag{23}$$

so that

$$G^{(2)}(t,t+\tau) = 4\Gamma_\beta^{(2)}(t,t+\tau). \tag{24}$$

As described earlier, the divergence of the δ functions is taken care of by filtering in a realistic experiment. The main distinction between these two approaches of measuring the

second-order coherence functions is how they are affected by noise in the experiment, as is discussed in the next section.

IV. REJECTION AND SUBTRACTION OF NOISE

The amplitude of microwave signals in a superconducting quantum circuit is small enough that amplifiers are essential for their observation, and so in a realistic experiment, the field is amplified *before* mixing. Using the Haus-Caves description of a quantum amplifier [34,43,44], an input operator $\hat{c}$ and an output operator $\hat{c}_{\rm amp}$ for a phase-preserving amplifier with gain g_c are related by

$$\hat{c}_{\rm amp} = \sqrt{g_c}\hat{c} + \sqrt{g_c - 1}\hat{h}_c^\dagger, \tag{25}$$

where $\hat{h}_c$ is an added noise mode.

It is clear that if $g_c > 1$ there will be added noise due to amplification, even at zero temperature. However, for thermal white Gaussian noise, one finds that all odd order moments vanish. As a result, the first moments of quadrature fields are not affected by this amplifier noise, just as they are not affected by vacuum noise. The contributions from other moments may be nonzero, however, and must be accounted for. For simplicity, we only consider the case of Gaussian white noise here, but similar results follow straightforwardly for general noise as long as the noise is independent of the inputs. Since the noise moments can be extracted from experimental data, the assumption of Gaussian noise is not essential.

The noise modes from different amplifiers are taken to commute, but in general they may be correlated. While the noise is normally taken to come from the amplification [34,43,44], formally one may also take $\hat{h}_c$ to include thermal noise from other sources, such as the vacuum ports of the IQ mixer and of the beam splitter, with only minor modifications. Here $\hat{h}_c$ is taken to have a commutator $[\hat{h}_c(t),\hat{h}_c^\dagger(t+\tau)] = \delta(\tau)$ in order to preserve the bosonic commutation relations of the amplified signals $\hat{c}_{\rm amp}$, and autocorrelation $\langle\hat{h}_c^\dagger(t)\hat{h}_c(t+\tau)\rangle = \bar{N}_c\delta(\tau)$. The noise sources are assumed to be independent of the inputs, so that $[\hat{c},\hat{h}_c] = [\hat{c},\hat{h}_c^\dagger] = 0$, and $\langle\hat{c}\hat{h}_c\rangle = \langle\hat{c}\hat{h}_c^\dagger\rangle = 0$. The correlations between $\hat{h}_c$ and the noise mode $\hat{h}_d$ from the other amplifier in the experiments described here is taken to be $\langle\hat{h}_c(t)\hat{h}_d^\dagger(t+\tau)\rangle = \bar{N}_{cd}\delta(\tau)$ while $\langle\hat{h}_c(t)\hat{h}_d(t+\tau)\rangle = 0$.

Using this noise model, one can calculate the different correlations $\Gamma^{(1)}_{\alpha,\beta}$ using the amplified modes, resulting in

$$\begin{aligned}\Gamma^{(1)}_{\alpha,{\rm amp}}(t,t+\tau) &= \frac{g_c}{2}G^{(1)}(t,t+\tau) + (\bar{N}_c + g_c)\delta(\tau),\\ \Gamma^{(1)}_{\beta,{\rm amp}}(t,t+\tau) &= \frac{\sqrt{g_c g_d}}{2}G^{(1)}(t,t+\tau) + \bar{N}_{cd}\delta(\tau),\end{aligned} \tag{26}$$

in the unfiltered case.

Since the thermal noise in the amplifiers is independent of the inputs, a steady-state experiment with the input mode $\hat{b}$ in the vacuum state can be used to estimate the noise strengths and subtract the corresponding terms from $\Gamma^{(1)}_{\alpha,\beta,{\rm amp}}$ to obtain an estimate of $G^{(1)}$. When the noise cross-correlation $\bar{N}_{cd}$ is expected to be zero or negligible compared to the noise auto-correlations $\bar{N}_c$ and $\bar{N}_d$, the approach to the estimation of $G^{(1)}$ based on $\Gamma^{(1)}_{\beta,{\rm amp}}$ provides *noise rejection* without additional postprocessing.

The second-order coherence function for the amplified fields has similar properties. One finds

$$\begin{aligned}&\Gamma^{(2)}_{\alpha,{\rm amp}}(t,t+\tau)\\ &= \frac{g_c g_d}{4}G^{(2)}(t,t+\tau) + \frac{g_c}{2}\delta(0)[g_d + \bar{N}_d]G^{(1)}(t,t)\\ &\quad + \frac{g_d}{2}\delta(0)[g_c + \bar{N}_c]G^{(1)}(t+\tau,t+\tau)\\ &\quad + \frac{\sqrt{g_c g_d}}{2}\bar{N}_{cd}\delta(\tau)[G^{(1)}(t+\tau,t) + G^{(1)}(t,t+\tau)]\\ &\quad + [g_c\bar{N}_d + g_c g_d + g_d\bar{N}_c]\delta^2(0)\\ &\quad + \langle\hat{h}_d^\dagger(t+\tau)\hat{h}_c^\dagger(t)\hat{h}_c(t)\hat{h}_d(t+\tau)\rangle,\end{aligned} \tag{27}$$

while

$$\begin{aligned}&\Gamma^{(2)}_{\beta,{\rm amp}}(t,t+\tau)\\ &= \frac{g_c g_d}{4}G^{(2)}(t,t+\tau) + \langle\hat{h}_d^\dagger(t+\tau)\hat{h}_d^\dagger(t)\hat{h}_c(t)\hat{h}_c(t+\tau)\rangle\\ &\quad + \frac{\sqrt{g_c g_d}}{2}\bar{N}_{cd}[\delta(\tau)G^{(1)}(t+\tau,t) + \delta(0)G^{(1)}(t+\tau,t+\tau)\\ &\quad + \delta(0)G^{(1)}(t,t) + \delta(\tau)G^{(1)}(t,t+\tau)],\end{aligned} \tag{28}$$

where all odd moments of the noise modes were taken to be zero (if such an assumption cannot be made, similar expressions involving the odd moments are easily derived but are omitted here for brevity). The recovery of the second-order coherence function from noisy signals is clearly more involved, but requires only the estimation of first-order coherence functions, as well as two- and four-point noise correlations in an experiment where the input mode $\hat{b}$ is prepared in the vacuum. Since the filters are taken to be linear and time invariant, $G^{(2)}_{\rm fil}$ is a scaled and distorted version of $G^{(2)}$, preserving the relative heights of the peaks, so that the nonclassical properties of the field can still be verified. Once again we see that $\Gamma^{(2)}_{\beta,{\rm amp}}$ provides a more direct estimation of $G^{(2)}$ by rejecting contributions from uncorrelated noise up to four-point noise correlations.

V. TWO-SIDED CAVITIES

Strictly speaking, the beam splitter is not necessary for the observation of the coherence functions described above. If one considers a two-sided cavity, illustrated in Fig. 5, the correlations between the cavity outputs behave in a manner similar to the outputs of the beam splitter in the HBT

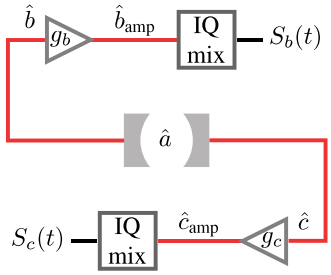

FIG. 5. (Color online) The setup for the observation of coherence functions using a two-sided cavity.

interferometers. In particular, using causality as well as the boundary conditions of the input and output fields of the two-sided cavity, Appendix E shows that

$$[\hat{b}_{\rm out}(t),\hat{c}^{\dagger}_{\rm out}(t')] = 0, \tag{29}$$

where $\hat{c}_{\rm out}$ is defined in a manner analogous to $\hat{b}_{\rm out}$, with a mirror leakage rate κ_c, and an amplifier with gain g_c being applied before mixing and measurement. It is thus possible to measure the complex envelopes of the two cavity outputs and calculate the correlations in the same manner as in the modified HBT setup without the need for an additional beam splitter. This can lead to simpler and smaller experimental setups, as beam splitters in the microwave regime can occupy a significant area in coplanar devices.

Calculating the correlations using the two cavity outputs $\hat{b}_{\rm out}$ and $\hat{c}_{\rm out}$ one finds

$$\Gamma^{(1)}_{\alpha,\rm amp}(t,t+\tau) = \kappa_c g_c G^{(1)}(t,t+\tau) + (\bar{N}_c + g_c)\delta(\tau), \tag{30}$$

$$\Gamma^{(1)}_{\beta,\rm amp}(t,t+\tau) = \sqrt{\kappa_b\kappa_c}\sqrt{g_c g_d}G^{(1)}(t,t+\tau) + \bar{N}_{bc}\delta(\tau), \tag{31}$$

$$\begin{aligned}\Gamma^{(2)}_{\alpha,\rm amp}(t,t+\tau) = {} & g_b g_c\kappa_b\kappa_c G^{(2)}(t,t+\tau) + [\bar{N}_b + g_b]\delta(0)g_c\kappa_c G^{(1)}(t,t) + [g_c + \bar{N}_c]\delta(0)g_b\kappa_b G^{(1)}(t+\tau,t+\tau)\\ & + \sqrt{g_b g_c}\sqrt{\kappa_b\kappa_c}\bar{N}_{bc}\delta(\tau)[G^{(1)}(t+\tau,t) + G^{(1)}(t,t+\tau)]\\ & + [g_b\bar{N}_c + g_b g_c + g_c\bar{N}_b]\delta^2(0) + \langle\hat{h}^{\dagger}_c(t+\tau)\hat{h}^{\dagger}_c(t)\hat{h}_b(t)\hat{h}_c(t+\tau)\rangle,\end{aligned} \tag{32}$$

$$\begin{aligned}\Gamma^{(2)}_{\beta,\rm amp}(t,t+\tau) = {} & g_b g_c\kappa_b\kappa_c G^{(2)}(t,t+\tau) + \langle\hat{h}^{\dagger}_b(t+\tau)\hat{h}^{\dagger}_b(t)\hat{h}_c(t)\hat{h}_c(t+\tau)\rangle\\ & + \sqrt{g_b g_c}\sqrt{\kappa_b\kappa_c}\bar{N}_{bc}\{\delta(\tau)[G^{(1)}(t+\tau,t) + G^{(1)}(t,t+\tau)] + \delta(0)[G^{(1)}(t+\tau,t+\tau) + G^{(1)}(t,t)]\},\end{aligned} \tag{33}$$

where $G^{(1)}$ and $G^{(2)}$ are now the coherence functions of the cavity field $\hat{a}$ instead of the cavity output fields, leading to the introduction of additional factors which depend on the cavity leakage rates $\kappa_{b,c}$. These expressions are directly analogous to Eqs. (26)–(28).

VI. SUMMARY

We have analyzed experiments for the measurement of field correlations using only field quadrature detectors and in the situation where the full record of many repetitions of the experiment is available. The combination of the quadrature measurements into complex envelopes gives direct access to antinormally ordered field correlations. While reordering of the operators in the correlations and the use of phase-preserving amplifiers introduces additional noise into these measurements, we demonstrated that the noise can be accounted for and subtracted in order to reveal only the field correlations of interest. Although there are indications that the number of statistical samples scales exponentially with the order of the correlation function, the measurement of low-order correlations is possible for current amplifier noise levels.

ACKNOWLEDGMENTS

M.P.S. was supported by the Natural Sciences and Engineering Research Council of Canada (NSERC). D.B. and A.W. were supported by the European Research Council and ETH Zurich. A.B. was supported by NSERC, the Alfred P. Sloan Foundation, and the Canadian Institute for Advanced Research.

APPENDIX A: INPUT STATE PREPARATION AND THERMAL EFFECTS

In order to demonstrate antibunching, it suffices to prepare cavity states of the form $|\psi\rangle = \alpha|0\rangle + \beta|1\rangle$. This can be achieved in circuit QED by following a two-step procedure. First, the qubit is prepared in a superposition $\alpha|g\rangle + \beta|e\rangle$ using a Rabi pulse. Second, the qubit state is mapped into the cavity state by bringing the qubit in resonance with the cavity. If the interaction time is half of a vacuum Rabi oscillation period, one obtains the mapping [45],

$$|g0\rangle \rightarrow |g0\rangle, \tag{A1}$$

$$|e0\rangle \rightarrow i|g1\rangle, \tag{A2}$$

$$|g1\rangle \rightarrow i|e0\rangle, \tag{A3}$$

$$|e1\rangle \rightarrow \cos\sqrt{2}\pi|e1\rangle + i\sin\sqrt{2}\pi|g2\rangle. \tag{A4}$$

This illustrates that the half-vacuum-period Rabi pulse only swaps the state between the qubit and the cavity only if there is a single excitation in the system. For states with more excitations, the vacuum Rabi frequency increases as $\sqrt{n}$, and a half-vacuum-period pulse leaves the system in an entangled state. As a result, assuming that the cavity starts out in the ground state, and that our system is described by

$$|\psi_0\rangle = |g\rangle \otimes |0\rangle, \tag{A5}$$

after the first Rabi pulse one obtains

$$|\psi_1\rangle = (\alpha|g\rangle + \beta|e\rangle) \otimes |0\rangle, \tag{A6}$$

$$\alpha = \cos(\theta_r/2), \tag{A7}$$

$$\beta = \sin(\theta_r/2), \tag{A8}$$

where θ_r is the Rabi angle, which is determined by the length of the Rabi pulse. Under the vacuum state assumption, the

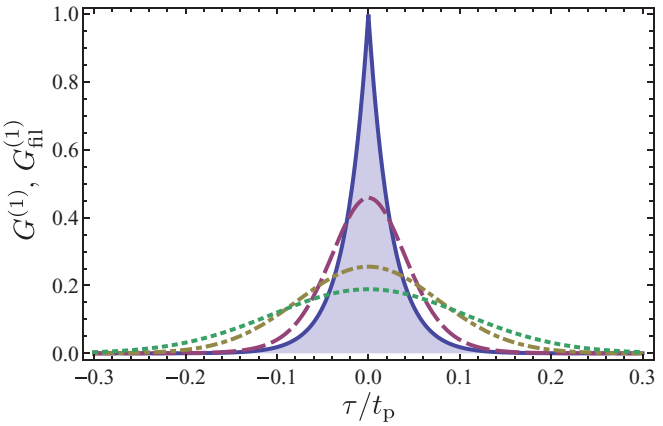

FIG. 6. (Color online) Distortion of the $e^{-\kappa\tau}$ pulses in $G^{(1)}(\tau)$ due to Gaussian filters of different bandwidths. The solid blue line is the unfiltered function, and the others are filtered bandwidth decreasing progressively: $31/t_p$ for the dashed purple line, $14/t_p$ for the dot-dashed yellow line, and $10/t_p$ for the dotted green line.

vacuum Rabi pulse swaps the qubit state and the cavity state, resulting in

$$|\psi_1\rangle = |g\rangle \otimes (\alpha|0\rangle + i\beta|1\rangle). \tag{A9}$$

Tracing out the qubit, the final cavity state is

$$|\psi_{f0}\rangle = \alpha|0\rangle + i\beta|1\rangle, \tag{A10}$$

$$\rho_{f0} = |\psi_{f0}\rangle\langle\psi_{f0}|. \tag{A11}$$

The coherence functions for various values of α and β are plotted in Figs. 6–8.

In the experiment [25] the assumption that the cavity is initially in the ground state is only approximately correct. Due to coupling to the input lines and the environment temperature, the cavity is always found in a thermal state with a small thermal photon number population. While this thermal field distribution has an observable influence in the measurement results, we disregard initial thermal excitations of the qubit because the effective temperature of the qubit is significantly lower than the effective temperature of the cavity.

To first order in the population of thermally excited photons, we take the equilibrium state of the cavity to be

$$p_0|0\rangle\langle 0| + p_1|1\rangle\langle 1|, \tag{A12}$$

where $p_{0,1}$ follow a truncated thermal distribution. Thus, it is necessary to consider the evolution of the system under the assumption that the cavity initially contains a single photon. In that case, one finds that the joint state of the qubit and cavity conditioned on the initial presence of a photon in the cavity to be

$$|\tilde{\psi}\rangle = i\alpha|e0\rangle + \beta\Gamma_c|e1\rangle + \beta\Gamma_s|g2\rangle, \tag{A13}$$

where

$$\Gamma_s = i\sin\sqrt{2}\pi, \tag{A14}$$

$$\Gamma_c = \cos\sqrt{2}\pi. \tag{A15}$$

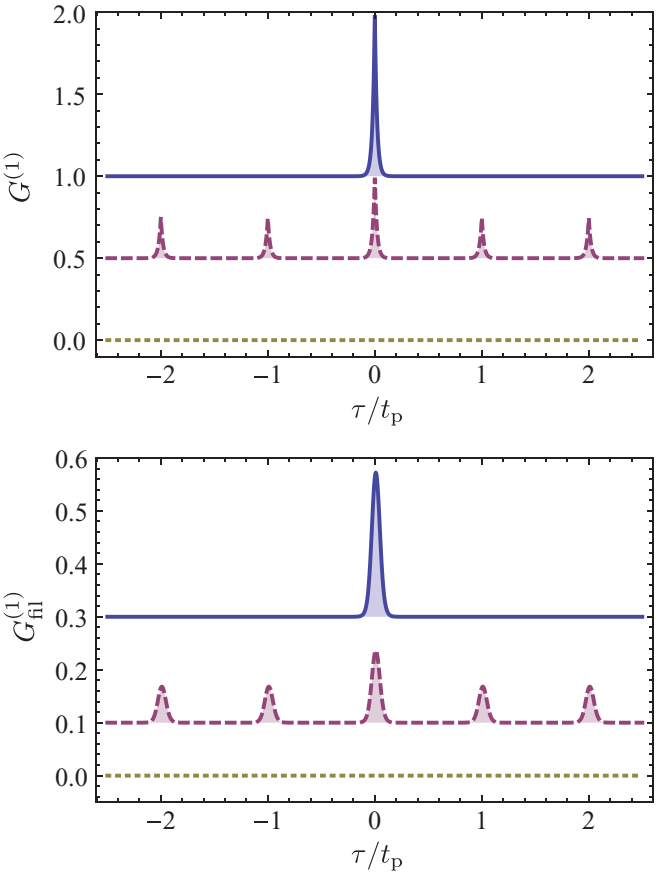

FIG. 7. (Color online) The pulse train for unfiltered $G^{(1)}(\tau)$ (top) and $G^{(1)}_{\rm fil}(\tau)$ after Gaussian filtering (bottom) under the periodic preparation of $|1\rangle$ (solid line), $\frac{1}{\sqrt{2}}(|0\rangle + |1\rangle)$ (dashed line), and $|0\rangle$ (dotted line). Each plot is offset for clarity, with the true value for the baseline being 0 in all cases. The Gaussian filter used here has a bandwidth of $31/t_p$.

Tracing out the qubit, the conditional cavity state is

$$\tilde{\rho}_f = |\alpha|^2(1-|\Gamma_c|^2)|0\rangle\langle 0| + |\Gamma_c|^2\rho_{f0} + |\beta\Gamma_s|^2|2\rangle\langle 2|. \tag{A16}$$

Combining this conditional state with the state conditioned on the cavity being in the vacuum states, and following the truncated thermal distribution, leads to the final cavity state,

$$\rho_f = (p_0 + |\Gamma_c|^2 p_1)\rho_{f0} + p_1(1-|\Gamma_c|^2)[|\alpha|^2|0\rangle\langle 0| + (1-|\alpha|^2)|2\rangle\langle 2|], \tag{A17}$$

and so it is clear that the correlation functions will be a statistical mixture of the correlation functions of the desired superposition $\alpha|0\rangle + i\beta|1\rangle$, the vacuum state, and the two-photon state $|2\rangle\langle 2|$. As long as p_1 is sufficiently small, it is still possible to observe $g^{(2)}(0) < g^{(2)}(kt_p)$ despite thermal excitations in the initial cavity state.

Moreover, note that in the case where $|\alpha|^2 \approx 1$, the final state of the cavity will have an enhanced vacuum component, no single-photon component, and a highly suppressed two-photon component, indicating that the cavity has been cooled by the half-vacuum-period Rabi pulse, as is observed in the experiment [25].

APPENDIX B: STATISTICAL ERROR ON CORRELATION FUNCTION ESTIMATES

In order to estimate the minimal number of repetitions of the experiment which must be performed to extract a given correlation function, consider the product of uncorrelated Gaussian random variables with zero mean and identical variances σ^2. These random variables correspond to the measurements of different outputs at steady state after the cavity state has decayed, and the variances are given by the noise power of the measurement record (including vacuum noise). In order to illustrate the argument, we consider real valued random variables V_i first, and generalize to complex valued random variables C_i. Since these random variables are uncorrelated, it follows that $\langle V_1 V_2 \cdots V_m \rangle = 0$. However, given a finite number of statistical samples, the sample average $\overline{V_1 V_2 \cdots V_m}$ will deviate from zero due to statistical fluctuations. Signal features which are comparable with the typical size of these fluctuations cannot be reliably observed. As the typical size of these fluctuations decreases with the increasing number of repetitions, this is in principle not a fundamental problem.

In order to estimate the number of samples needed for the reliable estimation of two-point correlations, consider the product of two Gaussian random variables. The characteristic function of this product is given by

$$\phi(U) = \int_{\mathbb{R}^3} dv_1\, dv_2\, du\; p_1(v_1) p_2(v_2) \delta(v_1 v_2 - u) e^{-iUu} \tag{B1}$$

$$= \frac{1}{\sqrt{1 + U^2 \sigma^4}}. \tag{B2}$$

The characteristic function of the average of R samples is given by

$$\phi_R(U) = \left[\phi\left(\frac{U}{n}\right) \right]^R. \tag{B3}$$

Given some error $\epsilon > 0$ and a number of repetitions R, the probability that the sample average $\overline{V_1 V_2}$ obeys $-\frac{\epsilon}{2} < \overline{V_1 V_2} < \frac{\epsilon}{2}$ is given by the integral of the inverse Fourier transform of $\phi_R(U)$ over this range and simplifies to

$$\Pr\left(|\overline{V_1 V_2}| < \frac{\epsilon}{2} \right) = \frac{1}{2\pi} \int_{-\infty}^{+\infty} dU\, \phi_R(U) \frac{\sin \frac{\epsilon U}{2}}{\frac{U}{2}}, \tag{B4}$$

which can be evaluated numerically. Thus, it is straightforward to calculate the number of repetitions R required to observe a feature larger than ϵ with confidence $\Pr(|\overline{V_1 V_2}| < \frac{\epsilon}{2})$.

Another approach that provides a looser bound, but is more readily generalized to higher-order correlations, is based on Chebyshev's inequality [46]. The variance of the product of independent random variables with zero mean is the product of the variances of each of the random variables. In the case of R samples of the product of m independent random variables V_i one finds that

$$\Pr\left(|\overline{V_1 V_2 \cdots V_m}| < \frac{\epsilon}{2} \right) > 1 - 4 \frac{\sigma^{2m}}{R \epsilon^2}. \tag{B5}$$

Note that in order to obtain this bound no assumption was made about the form of distribution of the random variables, other than the fact that the random variables are independent. Solving for R one obtains the worst-case upper bound,

$$R < \frac{4\sigma^{2m}}{\epsilon^2 \left[1 - \Pr\left(|\overline{V_1 V_2 \cdots V_m}| < \frac{\epsilon}{2} \right) \right]}, \tag{B6}$$

which makes clear the exponential relationship between the order of the correlation and the number of samples needed to have a statistical error of less than $\frac{\epsilon}{2}$ with some fixed probability.

In order to generalize this to complex-valued random variables C_i—where the real and imaginary parts of C_i are independent with variance σ, and the C_i are mutually independent—simply consider the real and imaginary parts of the correlations separately. In that case, because a larger number of terms contribute to the real and imaginary parts of the correlation, the variance has a larger bound, and one finds

$$R < \frac{8m\sigma^{2m}}{\epsilon^2 \Pr(\text{error})}, \tag{B7}$$

where Pr(error) is the probability that the absolute value of the real or imaginary parts of $\overline{C_1 C_2 \cdots C_m}$ are greater than $\frac{\epsilon}{2}$.

There is no indication that taking into account the Gaussian statistics of the random variables leads to better scalings. Thus the ratio of the number of statistical samples needed to estimate $G^{(2)}$ versus $G^{(1)}$ for some fixed noise variance and desired accuracy is at worse proportional to the noise power in the experiments. As a result, the noise added by the amplifier can be the crucial element in determining the feasibility of a correlation function experiment. It becomes even more important for higher-order correlations, where the number of samples depends on the noise power raised to some larger exponent.

APPENDIX C: COHERENCE FUNCTIONS FOR STATES WITH AT MOST ONE PHOTON

In the experiments described here [25], the cavity is periodically prepared in the state $\alpha|0\rangle + \beta|1\rangle$, with a period t_p such that $\kappa t_p \gg 1$. This ensures that, to a very good approximation, the cavity returns to the vacuum state before the superposition is prepared again.

The coherence functions can be calculated straightforwardly via their definitions in terms of the field correlations, while the correlations can be calculated by solving the Heisenberg equations of motion for the cavity field, and using the quantum regression theorem [34,47,48]. This procedure can be greatly simplified by noting that, if t and $t + \tau$ are in different preparation periods, then

$$\langle \hat{a}^\dagger(t) \hat{a}(t+\tau) \rangle = \langle \hat{a}^\dagger(t) \rangle \langle \hat{a}(t+\tau) \rangle, \tag{C1}$$

and

$$\langle \hat{a}^\dagger(t) \hat{a}^\dagger(t+\tau) \hat{a}(t+\tau) \hat{a}(t) \rangle = \langle \hat{a}^\dagger(t) \hat{a}(t) \rangle \langle \hat{a}^\dagger(t+\tau) \hat{a}(t+\tau) \rangle, \tag{C2}$$

due to the assumption $\kappa t_p \gg 1$.

In the case where t and $t + \tau$ are between $k t_p$ and $(k+1) t_p$ for some integer k, one finds that

$$\langle \hat{a}^\dagger(t) \hat{a}(t+\tau) \rangle = \langle \hat{n}(0) \rangle e^{-\kappa(t - k t_p - \tau/2)}, \tag{C3}$$

$$\langle \hat{a}^\dagger(t)\hat{a}^\dagger(t+\tau)\hat{a}(t+\tau)\hat{a}(t)\rangle = \langle \hat{a}^\dagger\hat{a}^\dagger\hat{a}\hat{a}\rangle e^{-\kappa(2t-2kt_p+\tau)}, \quad \text{(C4)}$$

while if t and $t+\tau$ are in different preparation periods starting at kt_p and $(k+l)t_p$, one finds that

$$\langle \hat{a}^\dagger(t)\hat{a}(t+\tau)\rangle = |\langle \hat{a}(0)\rangle|^2 e^{-\kappa[t-kt_p-(\tau-lt_p)/2]}, \quad \text{(C5)}$$

$$\langle \hat{a}^\dagger(t)\hat{a}^\dagger(t+\tau)\hat{a}(t+\tau)\hat{a}(t)\rangle = \langle \hat{n}(0)\rangle^2 e^{-\kappa(2t-2kt_p+\tau-lt_p)}. \quad \text{(C6)}$$

After integration over t, the first-order coherence function can be shown to be well approximated by

$$G^{(1)}(\tau) = \frac{1}{\kappa}\langle \hat{n}(0)\rangle e^{-\kappa|\tau|/2} + \frac{1}{\kappa}|\langle \hat{a}(0)\rangle|^2 \sum_{l\neq 0} e^{-\kappa|\tau-lt_p|/2}. \quad \text{(C7)}$$

This can be interpreted as a series of time-shifted copies of $e^{-\kappa|\tau|/2}$, where the peak centered at $\tau = 0$ has a height equal to $\langle n(0)\rangle$, while the peaks centered at nonzero multiples of t_p have a height equal to $|\langle a(0)\rangle|^2$.

Under similar assumptions, the second-order correlation function can be shown to be well approximated by

$$G^{(2)}(\tau) = \frac{1}{\kappa}\langle \hat{a}^\dagger(0)\hat{a}^\dagger(0)\hat{a}(0)\hat{a}(0)\rangle e^{-\kappa|\tau|} + \frac{1}{\kappa}\langle \hat{n}(0)\rangle^2 \sum_{l\neq 0} e^{-\kappa|\tau-lt_p|}, \quad \text{(C8)}$$

such that the center peak has a height proportional to $\langle \hat{a}^\dagger(0)\hat{a}^\dagger(0)\hat{a}(0)\hat{a}(0)\rangle$ while the other peaks have heights proportional to $\langle \hat{n}(0)\rangle^2$.

For the superpositions of vacuum and a single photon considered in [25], we find that

$$\langle \hat{n}(0)\rangle = |\beta|^2, \quad \text{(C9)}$$

$$|\langle \hat{a}(0)\rangle|^2 = |\alpha|^2|\beta|^2, \quad \text{(C10)}$$

$$\langle \hat{a}^\dagger(0)\hat{a}^\dagger(0)\hat{a}(0)\hat{a}(0)\rangle = 0, \quad \text{(C11)}$$

$$\langle \hat{n}(0)\rangle^2 = |\beta|^4, \quad \text{(C12)}$$

indicating that the center peak of $G^{(2)}$ is absent, while the other peaks are nonzero, which is a signature of the purely quantum effect known as antibunching [6,7].

APPENDIX D: FILTERING

The finite bandwidth of the detection chain can be modeled by considering the insertion of a bandpass filter in an ideal (infinite bandwidth) detection chain. In order to calculate the effect of filtering on correlation functions one can consider a general framework which describes what happens to multitime, multichannel correlations when measurement signals are filtered. Assume a system with n channels where each channel is filtered individually. One can write the filtered outcome of each channel $S_{\mathrm{fil},i}$ in terms of the input signal S_i and the filter function f_i by using the relations for linear time-invariant systems [49],

$$S_{\mathrm{fil},i}(t_i) = f_i(t_i) * S_i(t_i) \int_{-\infty}^{+\infty} f_i(\tau_i) S_i(t_i-\tau_i) d\tau_i. \quad \text{(D1)}$$

Each channel has a separate time variable t_i to capture the case of multitime correlations. This also clarifies with respect to which variable the convolution is done. The goal is now to express the filtered coherence function,

$$G_{\mathrm{fil}}(t_1,\ldots,t_n) = \langle S_{\mathrm{fil},1}(t_1)\, S_{\mathrm{fil},2}(t_2)\cdots S_{\mathrm{fil},n}(t_n)\rangle, \quad \text{(D2)}$$

in terms of the unfiltered coherence function,

$$G(t_1,\ldots,t_n) = \langle S_1(t_1)\, S_2(t_2)\cdots S_n(t_n)\rangle. \quad \text{(D3)}$$

This can be done straightforwardly by substituting Eq. (D1) into Eq. (D2),

$$G_{\mathrm{fil}}(t_1,\ldots,t_n) = \left\langle \prod_{i=1}^{n} f_i(t_i) * S_i(t_i) \right\rangle. \quad \text{(D4)}$$

Realizing that all convolutions are related to different time variables one can rearrange this expression as

$$G_{\mathrm{fil}}(t_1,\ldots,t_n) = f_1(t_1) * f_2(t_2) * \cdots f_n(t_n) * G(t_1,\ldots,t_n). \quad \text{(D5)}$$

The integral form clarifies this expression,

$$G_{\mathrm{fil}}(t_1,\ldots,t_n) = \int_{-\infty}^{+\infty} d\tau_1 \cdots \int_{-\infty}^{+\infty} d\tau_n\, f_1(t_1-\tau_1)\cdots \times f_n(t_n-\tau_n) G(\tau_1,\ldots,\tau_n). \quad \text{(D6)}$$

This expression can be seen as a generalized convolution with respect to more than one time variable. Introducing the global filter function,

$$F(t_1,\ldots,t_n) = f_1(t_1)\, f_2(t_2)\cdots f_n(t_n), \quad \text{(D7)}$$

one can write

$$G_{\mathrm{fil}}(t_1,\ldots,t_n) = F(t_1,\ldots,t_n) * G(t_1,\ldots,t_n). \quad \text{(D8)}$$

In the frequency domain, the same fact can be expressed by using the multidimensional Fourier transform instead, so that one may simply write

$$G_{\mathrm{fil}}(\omega_1,\ldots,\omega_n) = G(\omega_1,\ldots,\omega_n) F(\omega_1,\ldots,\omega_n). \quad \text{(D9)}$$

1. Two-point correlation functions

Using the spectral representation of some first-order coherence function $G(t_1,t_2)$ and the global filter function $F(t_1,t_2)$, one can write $G_{\mathrm{fil}}(\tau)$ as

$$G_{\mathrm{fil}}(\tau) = \int_{\mathbb{R}^3} dt\, d\omega_1\, d\omega_2\, e^{i(\omega_1+\omega_2)t + i\omega_2\tau} F(\omega_1,\omega_2) G(\omega_1,\omega_2), \quad \text{(D10)}$$

$$= \frac{1}{2\pi}\int_{-\infty}^{+\infty} d\omega\, e^{i\omega\tau} F(-\omega,\omega) G(-\omega,\omega). \quad \text{(D11)}$$

Considering the time representation of this expression, it is clear that the correlation function will be distorted by a convolution with the effective two-point correlation function $f_{\mathrm{eff}}(\tau) = \mathcal{F}\{F(-\omega,\omega)/2\pi\}$. Due to the linearity of the filters, one finds that Dirac δ functions in the noise correlations are replaced by f_{eff}, so that, for example,

$$\int_{\mathcal{I}} dt\, \langle \hat{h}_c^\dagger(t)\hat{h}_c(t+\tau)\rangle_{\mathrm{fil}} = \bar{N}_c f_{\mathrm{eff}}(\tau), \quad \text{(D12)}$$

where $h_c^{(\dagger)}(t)$ have been introduced in Eq. (25) and $\langle\cdot\rangle_{\mathrm{fil}}$ indicates that the average is taken over filtered outputs.

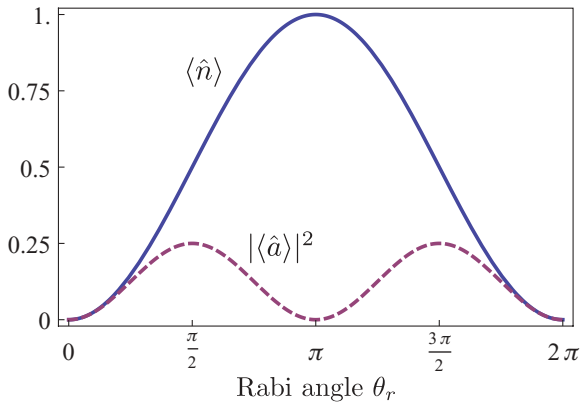

FIG. 8. (Color online) The heights of the center peak (solid line) and the side peaks (dashed line) of $G^{(1)}(\tau)$ as a function of the Rabi angle of the prepared state.

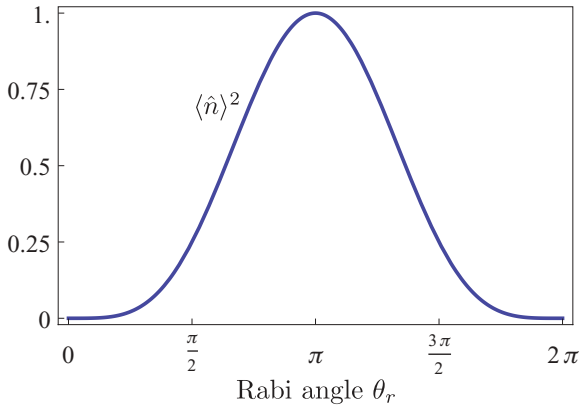

FIG. 10. (Color online) The heights of the side peaks (solid line) of $G^{(2)}(\tau)$ as a function of the Rabi angle of the prepared state. For the states considered here, the center peak is always zero.

This illustrates why the values for the different second-order coherence functions remain finite. Moreover, the other time-integrated two-point correlations are replaced by the convolution of the two-point correlation function with the $f_{\rm eff}$.

Note that since a linear time-independent filter is used, the relative heights of the peaks remain unchanged—only their shape gets distorted and scaled. This is illustrated in Figs. 6 and 7. The heights of the peaks for all superpositions of vacuum and a single photon are illustrated in Fig. 8.

2. Four-point correlation functions

We have seen previously that, in the absence of filters, $G^{(2)}$ takes the form of a train of pulses, as is illustrated in Fig. 9. For superpositions of vacuum and a single photon, the center peak is always absent, and the side peaks depend on the square of the mean photon number, as illustrated in Fig. 10.

Considering the second-order coherence function with filtered signals, one obtains

$$G^{(2)}_{\rm fil}(\tau) = \int_{\mathbb{R}^5} dt\, d\omega_1 \cdots d\omega_4 e^{i(\omega_1+\omega_2+\omega_3+\omega_4)t} e^{i(\omega_2+\omega_4)\tau} \times F(\omega_1,\omega_2,\omega_3,\omega_4) G^{(2)}(\omega_1,\omega_2,\omega_3,\omega_4). \quad \text{(D13)}$$

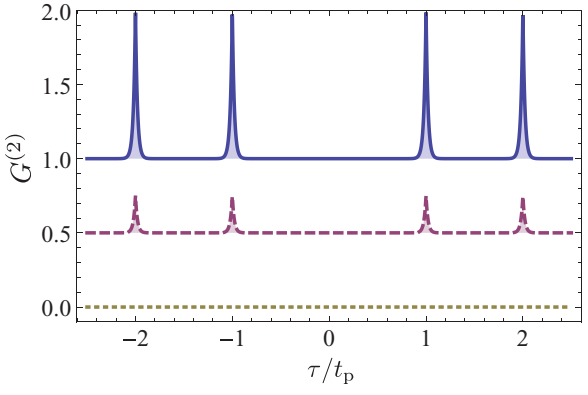

FIG. 9. (Color online) The pulse train for unfiltered $G^{(2)}(\tau)$ (top) under the periodic preparation of $|1\rangle$ (solid line), $\frac{1}{\sqrt{2}}(|0\rangle+|1\rangle)$ (dashed line), and $|0\rangle$ (dotted line). Each plot is offset for clarity, with the true value for the baseline being 0 in all cases.

The different types of correlations discussed simply determine the labeling of the variables. Applying a change of variables and integrating over time, one obtains

$$G^{(2)}_{\rm fil}(\tau) = \frac{1}{8\pi}\int_{-\infty}^{+\infty} d\Omega_2\, d\Omega_3\, d\Omega_4\, e^{-i\Omega_2\tau} \times F\left(\frac{-\Omega_2+\Omega_4}{2}, \frac{\Omega_2+\Omega_3}{2}, \frac{\Omega_2-\Omega_3}{2}, \frac{-\Omega_2-\Omega_4}{2}\right) \times G^{(2)}\left(\frac{-\Omega_2+\Omega_4}{2}, \frac{\Omega_2+\Omega_3}{2}, \frac{\Omega_2-\Omega_3}{2}, \frac{-\Omega_2-\Omega_4}{2}\right). \quad \text{(D14)}$$

Note that this leads to different behavior, in the sense that the correlation function is not simply convolved with an effective impulse response.

APPENDIX E: COMMUTATION RELATIONS OF TWO-SIDED CAVITY OUTPUTS

Taking both cavity mirrors to be leaky, one finds an additional boundary condition in the input-output description of the cavity [2,32–34],

$$\hat{c}_{\rm out} = \sqrt{\kappa_c}\hat{a} - \hat{c}_{\rm in}, \quad \text{(E1)}$$

where the $\hat{c}_{\rm in,out}$ modes are now the modes coupling to the second leaky mirror. The equation of motion [Eq. (9)] for $\hat{a}$ in the rotating frame then becomes

$$\dot{\hat{a}} = -\frac{\kappa_b+\kappa_c}{2}\hat{a} + \sqrt{\kappa_b}\hat{b}_{\rm in} + \sqrt{\kappa_c}\hat{c}_{\rm in}. \quad \text{(E2)}$$

From Eqs. (5) and (E1), one finds

$$[\hat{b}_{\rm out}(t),\hat{c}^\dagger_{\rm out}(t')] = \sqrt{\kappa_b\kappa_c}[\hat{a}(t),\hat{a}^\dagger(t')] - \sqrt{\kappa_b}[\hat{a}(t),\hat{c}^\dagger_{\rm in}(t')] - \sqrt{\kappa_c}[\hat{b}_{\rm in}(t),\hat{a}^\dagger(t')], \quad \text{(E3)}$$

where the input field operators were taken to commute. Integrating the solution for the equations of motion of the modes $\hat{b}(\omega,t)$ of the left transmission line and the modes $\hat{c}(\omega,t)$

of the right transmission line, and using the definition of the input fields, one obtains

$$\hat{b}_{\rm in}(t) = -\frac{\sqrt{\kappa_b}}{2}\hat{a}(t) + \frac{1}{\sqrt{2\pi}}\int_{-\infty}^{+\infty} d\omega \hat{b}(\omega,t),$$
$$\hat{c}_{\rm in}(t) = -\frac{\sqrt{\kappa_c}}{2}\hat{a}(t) + \frac{1}{\sqrt{2\pi}}\int_{-\infty}^{+\infty} d\omega \hat{c}(\omega,t). \quad \text{(E4)}$$

From causality and the boundary conditions above, one finds [34]

$$[\hat{a}(t),\hat{b}_{\rm in}(t')] = 0, \quad [\hat{a}(t),\hat{c}_{\rm in}(t')] = 0 \quad \text{for } t' > t, \quad \text{(E5)}$$
$$[\hat{a}(t),\hat{b}_{\rm out}(t')] = 0, \quad [\hat{a}(t),\hat{c}_{\rm out}(t')] = 0 \quad \text{for } t' < t. \quad \text{(E6)}$$

Combining these commutation relations with the input field definitions, one finally finds

$$[\hat{a}(t),\hat{c}^\dagger_{\rm in}(t')] = \sqrt{\kappa_c}u(t-t')[\hat{a}(t),\hat{a}^\dagger(t')],$$
$$[\hat{b}_{\rm in}(t),\hat{a}^\dagger(t')] = \sqrt{\kappa_b}u(t'-t)[\hat{a}(t),\hat{a}^\dagger(t')], \quad \text{(E7)}$$

where

$$u(t) = \begin{cases} 1, & t > 0 \\ \frac{1}{2}, & t = 0 \\ 0, & t < 0 \end{cases} \quad \text{(E8)}$$

and therefore

$$[\hat{b}_{\rm out}(t),\hat{c}^\dagger_{\rm out}(t')] = 0, \quad \text{(E9)}$$

as claimed.

[1] L. Mandel and E. Wolf, *Optical Coherence and Quantum Optics*, 1st ed. (Cambridge University Press, Cambridge, 2008).
[2] D. Walls and G. J. Milburn, *Quantum Optics*, 2nd ed. (Springer, New York, 2008).
[3] R. J. Glauber, Phys. Rev. Lett. **10**, 84 (1963).
[4] R. J. Glauber, Phys. Rev. **130**, 2529 (1963).
[5] L. Mandel and E. Wolf, Rev. Mod. Phys. **37**, 231 (1965).
[6] H. Paul, Rev. Mod. Phys. **54**, 1061 (1982).
[7] L. Davidovich, Rev. Mod. Phys. **68**, 127 (1996).
[8] C. Kurtsiefer, S. Mayer, P. Zarda, and H. Weinfurter, Phys. Rev. Lett. **85**, 290 (2000).
[9] Z. Yuan, B. E. Kardynal, R. M. Stevenson, A. J. Shields, C. J. Lobo, K. Cooper, N. S. Beattie, D. A. Ritchie, and M. Pepper, Science **295**, 102 (2002).
[10] M. Keller, B. Lange, K. Hayasaka, W. Lange, and H. Walther, Nature (London) **431**, 1075 (2004).
[11] K. M. Birnbaum, A. Boca, R. Miller, A. D. Boozer, T. E. Northup, and H. J. Kimble, Nature (London) **436**, 87 (2005).
[12] M. Hijlkema, B. Weber, H. P. Specht, S. C. Webster, A. Kuhn, and G. Rempe, Nat. Phys. **3**, 253 (2007).
[13] A. Wallraff, D. I. Schuster, A. Blais, L. Frunzio, R.-S. Huang, J. Majer, S. Kumar, S. M. Girvin, and R. J. Schoelkopf, Nature (London) **431**, 162 (2004).
[14] D. I. Schuster *et al.*, Nature (London) **445**, 515 (2007).
[15] A. Wallraff, D. I. Schuster, A. Blais, J. M. Gambetta, J. Schreier, L. Frunzio, M. H. Devoret, S. M. Girvin, and R. J. Schoelkopf, Phys. Rev. Lett. **99**, 050501 (2007).
[16] A. A. Houck *et al.*, Nature (London) **449**, 328 (2007).
[17] O. Astafiev, K. Inomata, A. O. Niskanen, T. Yamamoto, Y. A. Pashkin, Y. Nakamura, and J. S. Tsai, Nature (London) **449**, 588 (2007).
[18] M. Hofheinz, E. M. Weig, M. Ansmann, R. C. Bialczak, E. Lucero, M. Neeley, A. D. O'Connell, H. Wang, J. M. Martinis, and A. N. Cleland, Nature (London) **454**, 310 (2008).
[19] J. M. Fink, M. Göppl, M. Baur, R. Bianchetti, P. J. Leek, A. Blais, and A. Wallraff, Nature (London) **454**, 315 (2008).
[20] C. A. Regal, J. D. Teufel, and K. W. Lehnert, Nat. Phys. **4**, 555 (2008).
[21] M. A. Castellanos-Beltran, K. D. Irwin, G. C. Hilton, L. R. Vale, and K. W. Lehnert, Nat. Phys. **4**, 929 (2008).
[22] M. Hofheinz *et al.*, Nature (London) **459**, 546 (2009).
[23] O. Astafiev, A. M. Zagoskin, A. A. Abdumalikov, Y. A. Pashkin, T. Yamamoto, K. Inomata, Y. Nakamura, and J. S. Tsai, Science **327**, 840 (2010).
[24] N. B. Grosse, T. Symul, M. Stobinska, T. C. Ralph, and P. K. Lam, Phys. Rev. Lett. **98**, 153603 (2007).
[25] D. Bozyigit *et al.*, Nat. Phys. (to appear), e-print arXiv:1002.3738.
[26] M. Mariantoni, M. J. Storcz, F. K. Wilhelm, W. D. Oliver, A. Emmert, A. Marx, R. Gross, H. Christ, and E. Solano, e-print arXiv:cond-mat/0509737.
[27] E. P. Menzel, F. Deppe, M. Mariantoni, M. A. A. Caballero, A. Baust, T. Niemczyk, E. Hoffmann, A. Marx, E. Solano, and R. Gross, e-print arXiv:1001.3669.
[28] M. Mariantoni, E. P. Menzel, F. Deppe, M. A. A. Caballero, A. Baust, T. Niemczyk, E. Hoffmann, E. Solano, A. Marx, and R. Gross, e-print arXiv:1003.3194 (2010).
[29] J. M. Raimond, M. Brune, and S. Haroche, Rev. Mod. Phys. **73**, 565 (2001).
[30] H. Mabuchi and A. C. Doherty, Science **298**, 1372 (2002).
[31] A. Blais, R.-S. Huang, A. Wallraff, S. M. Girvin, and R. J. Schoelkopf, Phys. Rev. A **69**, 062320 (2004).
[32] M. J. Collett and C. W. Gardiner, Phys. Rev. A **30**, 1386 (1984).
[33] C. W. Gardiner and M. J. Collett, Phys. Rev. A **31**, 3761 (1985).
[34] C. Gardiner and P. Zoller, *Quantum Noise*, 3rd ed. (Springer, New York, 2004).
[35] H.-A. Bachor and T. C. Ralph, *A Guide to Experiments in Quantum Optics*, 2nd ed. (Wiley-VCH, New York, 2004).
[36] J. Gabelli, L.-H. Reydellet, G. Fève, J.-M. Berroir, B. Plaçais, P. Roche, and D. C. Glattli, Phys. Rev. Lett. **93**, 056801 (2004).
[37] D. M. Pozar, *Microwave Engineering*, 3rd ed. (Wiley, New York, 2004).
[38] A. Lupaşcu, E. F. C. Driessen, L. Roschier, C. J. P. M. Harmans, and J. E. Mooij, Phys. Rev. Lett. **96**, 127003 (2006).
[39] J. D. Teufel, T. Donner, M. A. Castellanos-Beltran, J. W. Harlow, and K. W. Lehnert, Nature Nanotech. **4**, 820 (2009).
[40] W. P. Schleich, *Quantum Optics in Phase Space*, 1st ed. (Wiley-VCH, New York, 2001).

[41] K. Husimi, Proc. Phys. Math. Soc. Jpn. **22**, 264 (1940).
[42] Y. Kano, J. Math. Phys. **6**, 1913 (1965).
[43] A. A. Clerk, M. H. Devoret, S. M. Girvin, F. Marquardt, and R. J. Schoelkopf, Rev. Mod. Phys. **82**, 1155 (2010).
[44] C. M. Caves, Phys. Rev. D **26**, 1817 (1982).
[45] Y. Yamamoto and A. Imamoglu, *Mesoscopic Quantum Optics* (Wiley-Interscience, New York, 1999).
[46] J. S. Rosenthal, *A First Look at Rigorous Probability Theory*, 2nd ed. (World Scientific, Singapore, 2009).
[47] M. Lax, Phys. Rev. **129**, 2342 (1963).
[48] H. Carmichael, *An Open Systems Approach to Quantum Optics* (Springer, New York, 1993).
[49] J. G. Proakis and D. K. Manolakis, *Digital Signal Processing*, 4th ed. (Prentice Hall, Upper Saddle River, 2006).